North Atlantic Intermediate Depth Variability During the Younger Dryas: Evidence From Benthic Foraminiferal Mg/Ca and the GFDL R30 Coupled Climate Model

Rosemarie E. Came[1,2], William B. Curry[3], Delia W. Oppo[3], Anthony J. Broccoli[4], Ronald J. Stouffer[5], and Jean Lynch-Stieglitz[6]

Two new records of paired benthic foraminiferal Mg/Ca and $\delta^{18}O$ from two low latitude western Atlantic sediment cores—one taken from within the Florida Current and the other from the Little Bahama Bank—provide insights into the spatial distribution of intermediate depth temperature and salinity variability during the deglaciation. During the Younger Dryas cold event, both temperature and salinity increased at the Florida Current site and decreased at the Little Bahama Bank site. The temperature increase within the Florida Current is consistent with a reduction in the strength of the northward-moving surface return flow of the Atlantic meridional overturning circulation; the temperature decrease at the Little Bahama Bank is consistent with a cooling of high latitude North Atlantic surface waters. To test the possibility that a freshening of the surface North Atlantic caused the paleoceanographic changes during the Younger Dryas, the Geophysical Fluid Dynamics Laboratory (GFDL) R30 coupled ocean-atmosphere general circulation model was forced using a North Atlantic freshwater perturbation of 0.1 Sv for a period of 100 years. The freshwater flux causes an overall reduction in the Atlantic overturning from 25 Sv to 13 Sv. However, at ~1,100 m water depth, ventilation increases, causing decreases in both temperature and salinity throughout much of the intermediate depth, open-ocean North Atlantic. At the western boundary, intermediate depth temperatures and salinities increase due to weakened overturning, and also due to an increase in runoff from the Amazon River, which causes a surface stability and a decrease in the upwelling of colder, deeper waters.

[1]Massachusetts Institute of Technology/Woods Hole Oceanographic Institution Joint Program in Oceanography, Woods Hole, Massachusetts, USA.
[2]Present address: Division of Geological and Planetary Sciences, California Institute of Technology, Pasadena, California, USA.
[3]Department of Geology and Geophysics, Woods Hole Oceanographic Institution, Woods Hole, Massachusetts, USA.
[4]Department of Environmental Sciences, Rutgers University, New Brunswick, New Jersey, USA.
[5]NOAA Geophysical Fluid Dynamics Laboratory, Princeton, New Jersey, USA.
[6]School of Earth and Atmospheric Sciences, Georgia Institute of Technology, Atlanta, Georgia, USA.

Ocean Circulation: Mechanisms and Impacts
Geophysical Monograph Series 173

10.1029/173GM16

INTRODUCTION

The transition from the most recent glaciation to the Holocene interglacial was punctuated by several millennial scale climate oscillations [*Bond et al.*, 1993; *Dansgaard et al.*, 1993; 1992]. The most dramatic of these oscillations was the Younger Dryas, which was a near-glacial cold event in the North Atlantic that lasted from ~13,000 to ~11,500 years before present. Many paleoclimate records from the circum-North Atlantic reveal a significant cooling during the Younger Dryas, including oxygen isotopes in Greenland ice cores [*Dansgaard*, 1984] and the faunal assemblages of planktic foraminifera [*Ruddiman and McIntyre*, 1981]. More recently, however, the widespread nature of the event has been revealed in paleoclimate records from around the globe,

including sea surface temperatures in the Cariaco Basin [*Lea et al.*, 2003], Asian monsoon intensity recorded in speleothems from Hulu Cave, eastern China [*Wang et al.*, 2001], and high altitude temperatures recorded in Bolivian ice cores [*Thompson et al.*, 1998].

A freshwater-induced reduction in the Atlantic meridional overturning circulation (MOC) is often invoked as a potential cause or amplifier of the high latitude cooling during the Younger Dryas [*Broecker et al.*, 1989; *Keigwin et al.*, 1991; *Tarasov and Peltier*, 2005]. Model simulations suggest that such a decrease in overturning would cause a cooling of surface waters in high northern latitudes, and a warming of surface and thermocline waters in lower latitudes [*Manabe and Stouffer*, 1997; *Marchal et al.*, 1999; *Rahmstorf*, 1994; *Rühlemann et al.*, 2004; *Stouffer et al.*, 2006; *Zhang and Delworth*, 2005]. Alkenone-derived temperature estimates from the open-ocean, western tropical Atlantic suggest that a low latitude surface warming occurred during the Younger Dryas, with sea surface temperatures increasing by 1.2°C [*Rühlemann et al.*, 1999]. Foraminiferal Mg/Ca temperature estimates from another western tropical Atlantic site (North Brazil Current) confirm this tropical sea surface warming [*Weldeab et al.*, 2006]. However, Mg/Ca-derived sea surface temperatures from the Cariaco Basin off Northern Venezuela suggest a cooling of 3 to 4°C [*Lea et al.*, 2003], although temperature variability at this location may reflect changes in local upwelling.

Ice-rafted debris in sediment cores from the North Atlantic [*Bond et al.*, 1993; *Bond and Lotti*, 1995] and from the shelf east of the Hudson Strait [*Andrews et al.*, 1995] suggest an increase in the flux of icebergs into the North Atlantic during the Younger Dryas event, providing a mechanism for freshwater forcing. However, a difficulty with the freshwater forcing hypothesis is that the onset of the Younger Dryas cooling does not coincide with documented North Atlantic freshwater pulses, leading to investigations of Southern Ocean forcing mechanisms. Recent modeling studies suggest that increased freshwater into the surface of the Southern Ocean intensifies the transformation of dense Circumpolar Deep Water (CDW) into the lighter Antarctic Intermediate Water (AAIW) [*Saenko et al.*, 2003b], which then feeds the return flow of North Atlanic Deep Water (NADW) formation [*Gordon*, 1986], and intensifies the MOC. It has been suggested that meltwater pulse 1a into the Southern Ocean caused this type of North Atlantic MOC intensification, and led to the Bølling-Allerød warming in the North Atlantic region [*Weaver et al.*, 2003]. A Southern Ocean forcing mechanism predicts a very different Atlantic subsurface water mass distribution for abrupt climate events like the Younger Dryas: in the "off" circulation mode, NADW is less dense than AAIW, creating a stagnant, poorly ventilated, upper North Atlantic Ocean [*Keeling and Stephens*, 2001; *Saenko et al.*, 2003a].

Foraminiferal nutrient proxies, such as $\delta^{13}C$ and Cd_W, are often used to reconstruct water mass distributions in the subsurface Atlantic Ocean. Nutrient evidence from the last glacial reveals a subsurface geometry in which the influence of NADW decreased, and the influence of North Atlantic Intermediate Water (NAIW) increased [*Boyle and Keigwin*, 1987; *Duplessy et al.*, 1988; *Oppo and Lehman*, 1993]. For the Younger Dryas, nutrient evidence [*Boyle and Keigwin*, 1987; *Marchitto et al.*, 1998; *Zahn and Stüber*, 2002] suggests a subsurface geometry that was similar to that of the last glacial, although the contribution of NAIW into the South Atlantic may have decreased relative to the glacial [*Came et al.*, 2003]. Benthic-planktic radiocarbon pairs [*Keigwin*, 2004] and Pa/Th evidence [*McManus et al.*, 2004] confirm the glacial-like subsurface geometry for the Younger Dryas, although other evidence suggests a Younger Dryas subsurface geometry that was similar to the modern [*Sarnthein et al.*, 2001].

Benthic foraminiferal oxygen isotopes have been used as a tracer of bottom water temperatures (BWT) during the Younger Dryas, and the results compared with temperature anomalies from freshwater forcing simulations using zonally averaged models [*Rühlemann et al.*, 2004]. One complication with this approach is that both seawater $\delta^{18}O$ ($\delta^{18}O_{sw}$) and calcification temperature influence the $\delta^{18}O$ of foraminifera, making the interpretation of foraminiferal $\delta^{18}O$ as a BWT proxy uncertain. Furthermore, zonally averaged models cannot reveal the spatial complexity of BWT variability across the Atlantic basin, and a single core location may not be representative of a zonal average.

In this study, we present downcore records of paired benthic foraminiferal Mg/Ca and $\delta^{18}O$ from two North Atlantic sediment cores, from which we determine both temperature and salinity. The two cores lie in key locations for detecting changes in intermediate depth water properties during the Younger Dryas: a core from the Little Bahama Bank, which monitors variability within the deeper, unventilated portion of the North Atlantic subtropical gyre [*Slowey and Curry*, 1995]; and a core from within the Florida Current, which monitors variability within the northward return flow of the MOC [*Lynch-Stieglitz et al.*, 1999].

In order to test the sensitivity of oceanographic properties to a freshening of the surface North Atlantic, the Geophysical Fluid Dynamics Laboratory R30 coupled ocean-atmosphere general circulation model (GFDL R30) was forced using a North Atlantic freshwater perturbation of 0.1 Sv for a period of 100 years [*Dahl et al.*, 2005]. The purpose of this study is to assess the response of the ocean's subsurface to a forcing that is consistent with freshwater estimates for the Younger Dryas [e.g. *Licciardi et al*., 1999]. The response is then compared to actual paleoceanographic evidence in an attempt to determine whether a North Atlantic freshwater perturbation is an adequate explanation for the observed changes during

the Younger Dryas. It should be noted, however, that the control integration of the GFDL R30 model, which is the base state for the freshwater perturbation experiment, is a simulation of modern conditions, not those of the deglacial, so the experiment should be viewed solely as a sensitivity study.

STUDY AREAS

Sediment core OCE205-2-100GGC (LBB) was taken from the flanks of the Little Bahama Bank, within the Northwest Providence Channel, at 26.06°N, 78.03°W, and 1,057 m water depth (Figure 1). Waters of the Northwest Providence Channel flow westward from the Sargasso Sea to the Straits of Florida [*Slowey and Curry*, 1995]. Today, depths above 1,000 m are bathed by waters of the wind-driven North Atlantic subtropical gyre, with the same temperature, salinity, and density structure as the western portion of the gyre [*Slowey and Curry*, 1995]. Waters below 1,000 m are fed by the upper component of NADW. These waters are poorly ventilated because they originate in the subpolar gyre, where residence times are long and wind driven upwelling occurs [*Jenkins*, 1980; *McCartney*, 1982; *Sarmiento et al.*, 1982]. Waters circulate within the subpolar gyre before entering the subtropical gyre at depth [*Jenkins*, 1980; *Luyten et al.*, 1983; *McCartney*, 1982; *Sarmiento et al.*, 1982].

Sediment core KNR166-2-31JPC (FC) was taken from within the Florida Current, just south of the Florida Keys, at 24.22°N, 83.30°W, and 751 m water depth (Figure 1). Today, waters of the FC are a mixture of recirculated North Atlantic subtropical gyre water (17 Sv) and intermediate depth southern source waters (13 Sv) [*Schmitz et al.*, 1993; *Schmitz and Richardson*, 1991]. At mid-depths (12-24°C temperature range), ~5% of the FC waters are of South Atlantic origin, but below 400 m, ~80% of the waters are of South Atlantic origin [*Schmitz and Richardson*, 1991]. The intermediate depth southern source waters that feed the FC are observed in the South Atlantic as a northward moving salinity minimum layer that originates near the Antarctic Polar Front. After these waters pass through the Florida Strait, they continue northward, feeding the Gulf Stream and the North Atlantic Current.

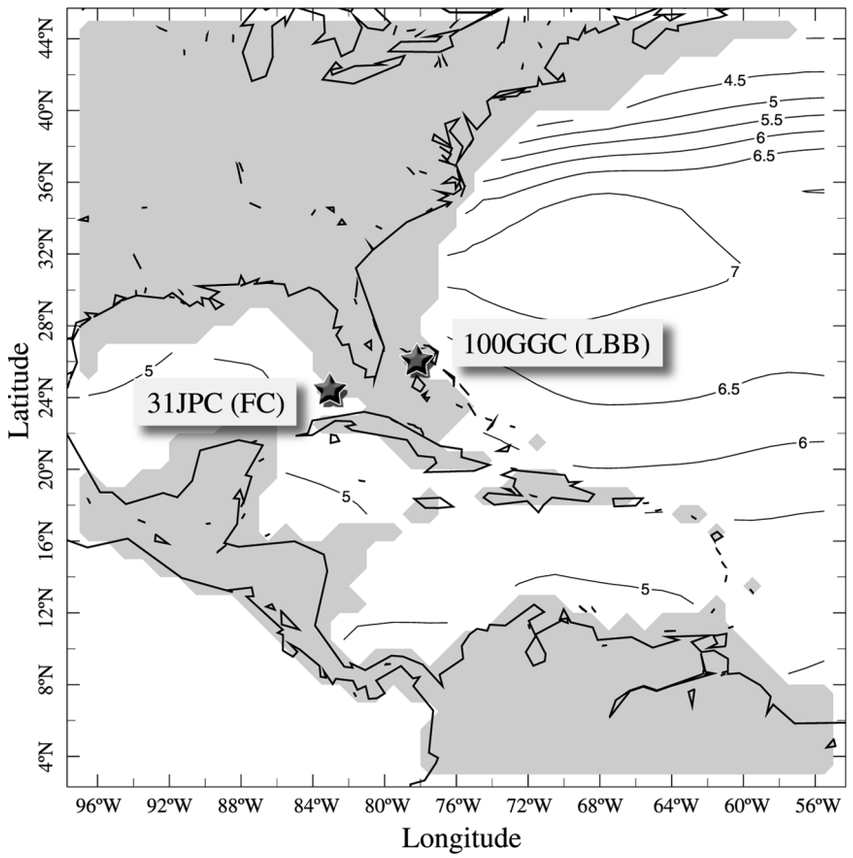

Figure 1. Map of the study area with mean annual temperatures at 1,000 m water depth [*Levitus and Boyer*, 1994] and the locations of OCE205-2-100GGC and KNR166-2-31JPC.

Today, intermediate depths at these two geographic locations have very different water properties. For example, mean annual temperatures at 1,000 m depth are about 1°C warmer at the LBB than at the FC [*Levitus and Boyer*, 1994]. However, since the FC core location is 300 m shallower than the LBB core location, BWT and salinities are very similar: approximately 5.35°C and 35.05 at LBB [*Slowey and Curry*, 1995], and 5.78°C and 34.90 at FC (measured during core collection, KNR166-2).

METHODS

Foraminiferal Elemental and Isotopic Analyses

We used previously published age models for both LBB and FC [*Came et al.*, 2007]. The age model for LBB included 13 accelerator mass spectrometer (AMS) radiocarbon dates obtained from the planktic foraminifer *Globigerinoides sacculifer*; and the age model for FC included eight AMS dates obtained from *G. sacculifer*, one from the planktic foraminifer *G. ruber*, and one from a mixture of *G. sacculifer* and *G. ruber*. AMS radiocarbon dates were converted to calendar age using the online calibration program Calib 5.02 [*Stuiver and Reimer*, 1993], the Marine04 calibration data set [*Hughen et al.*, 2004], and a reservoir correction of 400 years. The sedimentation rate for LBB is ~6 cm/kyr, with higher sedimentation rates in the more recent Holocene (~8 cm/kyr) and lower rates near the last glacial (~3 cm/kyr) (Figure 2a). The average sedimentation rate for FC is slightly higher than 8 cm/kyr (Figure 3a). The age model for the FC core did not include the calculated calendar age for 128 cm due to an apparent age reversal at that depth. The age reversal may indicate bioturbation or, if uncertainties in the reservoir correction are considered, it may indicate an increased

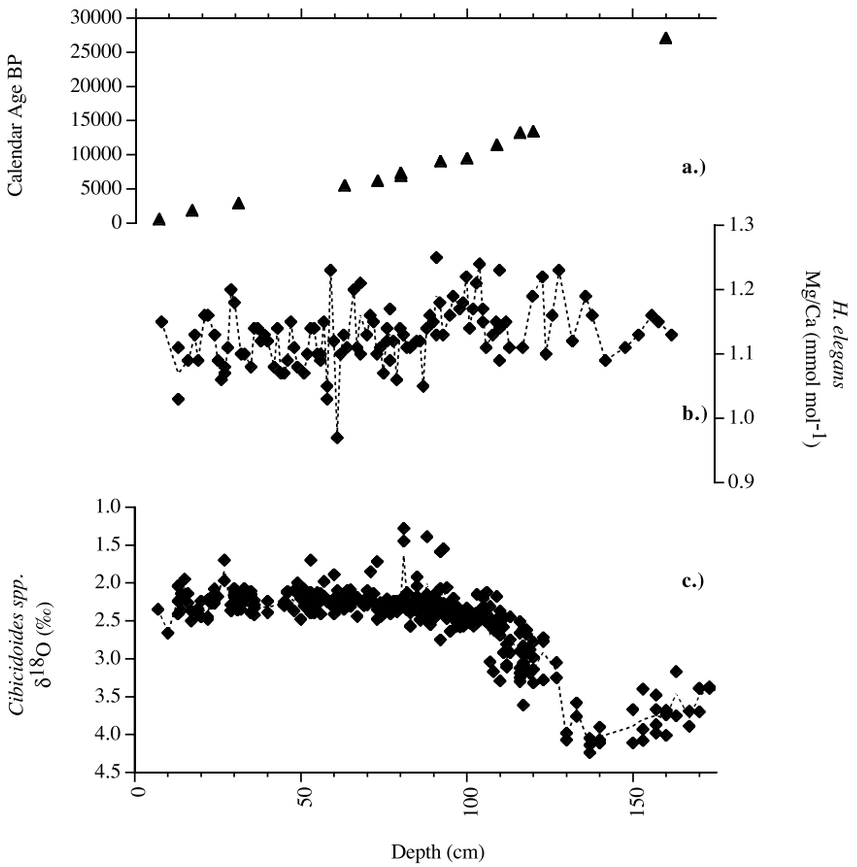

Figure 2. Benthic Mg/Ca and $\delta^{18}O$ data from OCE205-2-100GGC vs. depth: (a) AMS radiocarbon dates [*Came et al.*, 2007] converted to calendar age using Calib 5.02 [*Stuiver and Reimer*, 1993], the calibration data set of *Hughen et al*. [2004], and a reservoir correction of 400 years; (b) all *H. elegans* Mg/Ca; (c) all previously acquired *Cibicidoides* spp. $\delta^{18}O$ [*Slowey and Curry*, 1995] as well as newly acquired *Cibicidoides* spp. $\delta^{18}O$ [this paper].

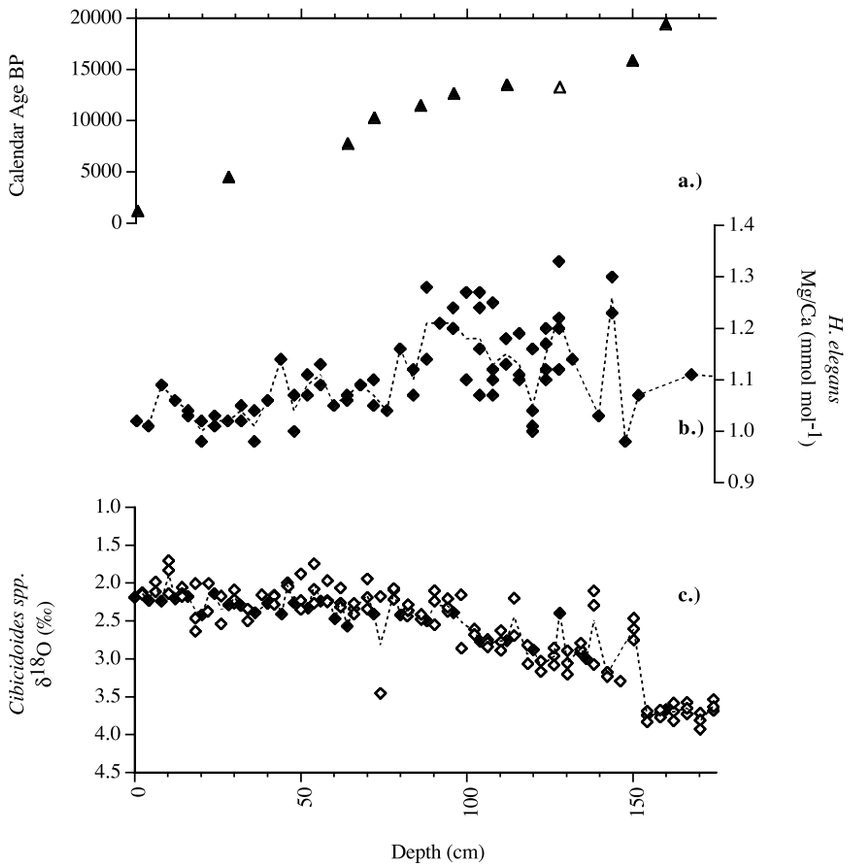

Figure 3. Benthic Mg/Ca and $\delta^{18}O$ data from KNR166-2-31JPC vs. depth: (a) AMS radiocarbon dates [*Came et al.*, 2007] converted to calendar age using Calib 5.02 [*Stuiver and Reimer*, 1993], the calibration data set of *Hughen et al*. [2004], and a reservoir correction of 400 years (open symbol was excluded from the age model); (b) all *H. elegans* Mg/Ca; (c) all *Cibicidoides* spp. $\delta^{18}O$. Open symbols in (c) represent analyses of individual foraminifers; closed symbols represent analyses of multiple individuals.

sedimentation rate and no bioturbation. In either case, the affected depth interval is significantly deeper in the core than the interval representing the Younger Dryas, so it does not affect our interpretation of the data.

Mg/Ca ratios were measured in the tests of the benthic foraminifer *Hoeglundina elegans*. Each sample consisted of approximately 2-3 individuals, which were crushed and cleaned according to the trace metal protocol [*Boyle and Keigwin*, 1985/6] with a reversal of the oxidative and reductive steps [*Boyle and Rosenthal*, 1996; *Rosenthal*, 1994; *Rosenthal et al.*, 1995]. Samples were dissolved in trace-metal-clean HNO_3 to obtain samples of approximately 200 ppm Ca. Mg/Ca ratios were measured using a Thermo-Finnigan Element2 sector field single collector ICP-MS following the method of *Rosenthal* [1999]. Mn/Ca and Al/Ca were also measured in order to monitor contamination due to manganese carbonate overgrowths and terrestrial input. Manganese carbonate overgrowths are a potential source of contamination in many species of benthic foraminifera [*Boyle*, 1983]. However, the species *H. elegans* was chosen for this study because it does not suffer from the contamination caused by such overgrowths [*Boyle et al.*, 1995].

Converting ICP-MS intensity ratios to elemental ratios using an external standard requires similar [Ca] in both the sample and the standard due to a calcium matrix effect. To correct for samples with varying [Ca], we ran a series of standards with identical element to Ca ratios, but with Ca concentrations that varied over the anticipated sample concentration range. The resulting matrix effect was calculated and the sample ratios were corrected. The corrections were less than ±0.03 mmol mol^{-1} Mg/Ca.

In order to assess the precision of measurements on the ICP-MS, three consistency standards were treated as samples in each of the runs in which the data were generated. Mean Mg/Ca values for the three consistency standards were 1.7 mmol mol^{-1}, 3.3 mmol mol^{-1} and 5.0 mmol mol^{-1}.

Standard deviations were ±0.02 mmol mol^{-1} (n = 9), ±0.03 mmol mol^{-1} (n = 9), and ±0.04 mmol mol^{-1} (n = 9), respectively. We converted Mg/Ca to temperature using the Mg/Ca-temperature calibration equations for *H. elegans* [*Rosenthal et al.*, 2006]:

for $[\Delta CO_3]_{aragonite} > 15$ μmol kg^{-1},

$$Mg/Ca = (0.034 \pm 0.002) \times BWT + (0.96 \pm 0.03); \quad (1)$$

for $[\Delta CO_3]_{aragonite} < 15$ μmol kg^{-1},

$$Mg/Ca = 0.034 \times BWT - (0.017 \pm 0.002) \times (15 - [\Delta CO_3]_{aragonite}) + 0.96, \quad (2)$$

where BWT is in °C and Mg/Ca is in mmol mol^{-1}. The $[\Delta CO_3]_{aragonite}$ is the level of aragonite saturation, which is defined by *Broecker and Peng* [1982] as:

$$[\Delta CO_3] = [CO_3]_{in\ situ} - [CO_3]_{saturation,} \quad (3)$$

where $[CO_3]$ is the carbonate ion concentration and $[CO_3]_{saturation} = 120\exp[0.16(Z - 4)]$, where Z is depth in kilometers and $[CO_3]$ is in μmol kg^{-1}. The resulting temperature error is ±1.2°C.

Samples used for oxygen isotopic analyses consisted of 1-4 individual tests of the benthic foraminiferal species *Cibicidoides* spp. at LBB [*Slowey and Curry*, 1995; this paper] and at FC. Oxygen isotopic data for core OCE205-2-100GGC were generated using a Finnigan-MAT 252 with Kiel II carbonate preparation device at the Woods Hole Oceanographic Institution (WHOI). Oxygen isotopic data for core KNR166-2-31JPC were generated using both a GV Optima with Multiprep at the Lamont-Doherty Earth Observatory, and a Finnigan-MAT 253 with Kiel III carbonate preparation device at WHOI. Analytical precision for oxygen isotopic analyses is ±0.08‰ (1σ).

Mg/Ca-derived temperatures and foraminiferal oxygen isotopic values were used to calculate $\delta^{18}O_{sw}$ using the conversion equation for *Cibicidoides* spp. [*Lynch-Stieglitz et al*., 1999]:

$$\delta^{18}O_{Cib} = [\delta^{18}O_{sw} - 0.27] - 0.21 \times BWT + 3.38. \quad (4)$$

Seawater $\delta^{18}O$ was not converted to salinity because the evolution of the $\delta^{18}O$-salinity relationship over time is not well constrained. However, using the modern relationship, a $\delta^{18}O_{sw}$ change of 0.1‰ equals a salinity change of about 0.2 [*Lynch-Stieglitz et al*., 1999].

Model Description

The GFDL R30 coupled climate model consists of an atmospheric general circulation model coupled to an oceanic general circulation model. The R30 model is similar to older GFDL models (the GFDL R15, for example), but differs in that it contains higher spatial resolution in both the atmospheric and ocean components. The model description is presented in *Delworth et al.* [2002], but a brief summary follows.

The atmospheric component of the model has a resolution of approximately 3.75° longitude by 2.25° latitude, with 14 unevenly spaced levels in the vertical. The model has a seasonal cycle of insolation. Insolation is prescribed at the top of the atmosphere, using a solar constant of 1365 W m^{-2}. Clouds occur in the model when the relative humidity of an air parcel exceeds a critical value, which varies with height. Precipitation occurs whenever the simulated moisture content of an air parcel exceeds saturation. Each land grid box has the capacity to collect 15 cm of precipitation. When the water content of the grid box exceeds 15 cm, the excess is treated as surface runoff, which instantly enters the ocean via a routing scheme that is based upon observed drainage patterns. Runoff usually enters the upper ocean grid box only, although large river inputs enter the top two grid levels and several adjacent grid boxes. This flux of continental runoff into the ocean alters ocean salinity and impacts the ocean circulation.

The ocean component of the model uses version 1.1 of the Modular Ocean Model. Resolution is 1.875° longitude by 2.25° latitude, with 18 unevenly spaced levels. The ocean model requires parameterization of sub grid scale momentum mixing [*Bryan and Lewis,* 1979] and sub grid scale heat and salt mixing along isopycnal surfaces [*Redi,* 1982]. The model uses a horizontal background diffusivity for temperature and salinity of 0.4×107 cm^2 s^{-1} and a horizontal viscosity of 1.2×109 cm^2 s^{-1}. Mixing at the grid scale occurs when neighboring grid boxes are statically unstable, at which point the temperature and salinity of the two boxes are completely mixed. The oceanic and atmospheric components of the coupled model interact once per day through fluxes of heat, water and momentum.

Initialization of the model involves an 80-year integration of the atmospheric component using modern boundary conditions, and then a several thousand-year integration of the oceanic component using surface forcings calculated from the atmospheric integration. The oceanic component is integrated until drifts in deep ocean temperature and salinity are acceptably small. Since the atmospheric and oceanic components are not perfectly balanced, flux adjustments are used to prevent long-term drift. The flux adjustment terms are computed prior to coupling of the oceanic and atmospheric components, and do not vary from one year to the next. Because they are independent of the climate state, the flux adjustments are unlikely to systematically dampen or amplify anomalies, which develop during the coupled model integration.

THE FRESHWATER EXPERIMENT

The current freshwater forcing experiment (the same experiment investigated by *Dahl et al.* [2005]) uses the 300th year of the control integration as its initial condition. During years 301-400, a freshwater perturbation of 0.1 Sv was input uniformly over the North Atlantic from 50°N to 70°N. The temperature of the freshwater perturbation was assumed to be identical to the local temperature of the mixed layer. Thus, the freshwater pulse directly affects surface water salinities, but does not directly affect surface water temperatures. The control integration of the GFDL R30 coupled climate model is designed to faithfully simulate modern conditions. A simulation using deglacial boundary conditions could yield different results.

BENTHIC FORAMINIFERAL Mg/Ca RESULTS

Average core top values for depths corresponding to the last 3 kyr are 1.12 mmol mol^{-1} at LBB and 1.04 mmol mol^{-1} at FC (Figures 2b and 3b). Using the Mg/Ca-temperature relationship for waters where $[\Delta CO_3]_{aragonite} > 15$ μmol kg^{-1} (Eqn 1, above) [*Rosenthal et al.*, 2006], the calculated coretop temperature at LBB (4.8°C) is consistent with the modern BWT of 5.35°C [*Slowey and Curry*, 1995]. However, using the same relationship for the FC site, the calculated coretop temperature (2.4°C) is significantly lower than the modern BWT of 5.78°C. The discrepancy between coretop temperature and BWT at the FC site may be due to the error associated with Mg/Ca analyses, or due to uncertainties in the benthic foraminiferal Mg/Ca temperature calibration. Alternatively, the discrepancy may be due to a lower level of aragonite saturation at the FC site. Today, waters in the Florida Strait are supersaturated with respect to aragonite [*T.M. Marchitto*, unpublished data], yet $[\Delta CO_3]_{aragonite}$ values do approach the threshold level of 15 μmol kg^{-1}. Conceivably, bottom waters at the FC core location have $[\Delta CO_3]_{aragonite}$ values that are slightly lower than 15 μmol kg^{-1}, or had $[\Delta CO_3]_{aragonite}$ values that were slightly lower than 15 μmol kg^{-1} during much of the Holocene. Therefore, we convert Mg/Ca to temperature using both Eqns 1 and 2 (Figure 4). Eqns 1 and 2 differ only in intercept, so the choice of equation affects the magnitude of the calculated temperature, but not the magnitude of temperature variability (ΔT) (Figure 4). For Eqn 2, we assume $[\Delta CO_3]_{aragonite}$ = 11 μmol kg^{-1}, which yields a BWT at 2.1 ka of 5.8°C, which is close to the modern BWT. At present, the uncertainties associated with the method, as well as uncertainties regarding the aragonite saturation state over the course of time, prevent conclusive calculations of paleotemperatures. Therefore, the temperature estimates presented here should be viewed as provisional.

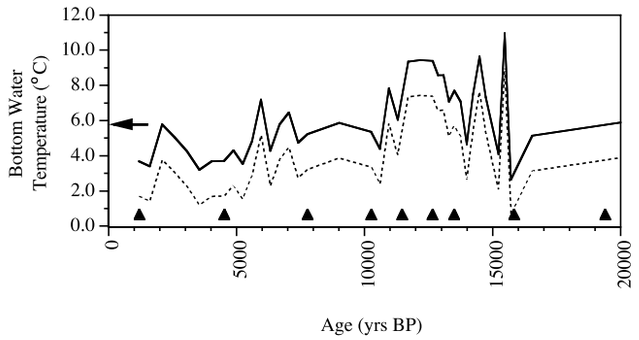

Figure 4. Mg/Ca-derived temperatures from KNR166-2-31JPC vs. calendar age. Dashed line uses the equation $Mg/Ca_{H.\ elegans} = 0.034$ BWT + 0.96 [*Rosenthal et al.*, 2006]; solid line uses the equation $Mg/Ca = 0.034\ BWT - (0.017 \pm 0.002) \times (15 - [\Delta CO_3]_{aragonite}) + 0.96$ [*Rosenthal et al.*, 2006], where $[\Delta CO_3]_{aragonite}$ is assumed to be 11 μmol kg^{-1}. Arrow at left marks the modern bottom water temperature of 5.78°C. Triangles are AMS dates converted to calendar age.

The mean benthic Mg/Ca data from the LBB site do not reveal a clear glacial-interglacial trend (Figure 2b; Plate 1b). Instead, similar temperatures of ~4°C and ~5°C are observed for the glacial (20.1 ka) and interglacial, respectively. However, pronounced suborbital variability is present in the record. At ~16 ka, Mg/Ca temperatures decreased by nearly 4°C, perhaps coincident with Heinrich event 1 (although sampling resolution and insufficient age control prevent conclusive identification of the event). At ~14.5 ka, coincident with the Bølling-Allerød warming in the high latitude North Atlantic, temperatures increased by ~4°C. At ~13 ka, coincident with the Bølling-Allerød to Younger Dryas cooling, temperatures decreased by ~3.5°C. At 10.4 ka, temperatures returned to pre-Younger Dryas values. By 8 ka, temperatures decreased to near modern values, where they remained for the rest of the Holocene.

Like LBB, the mean benthic Mg/Ca data from FC do not reveal a clear glacial-interglacial trend (Figure 3b; Plate 1b), but rather, similar temperatures of ~6.5°C and ~4.5°C for the glacial (~22 ka) and interglacial, respectively. Pronounced suborbital variability is also present in the FC record. Prior to ~14 ka, two dramatic temperature oscillations occurred (but again, sample resolution prevents reliable identification of events). At ~14 ka, temperatures began to increase in concert with the gradual cooling observed in the GISP2 ice core record [*Grootes et al.*, 1993]. Warmest temperatures (~9.5°C) occurred at ~12.5 ka, suggesting a Bølling-Allerød to Younger Dryas warming of nearly 5°C. By ~10.5 ka, temperatures returned to Bølling-Allerød-like values, and remained close to modern values for the remainder of the Holocene.

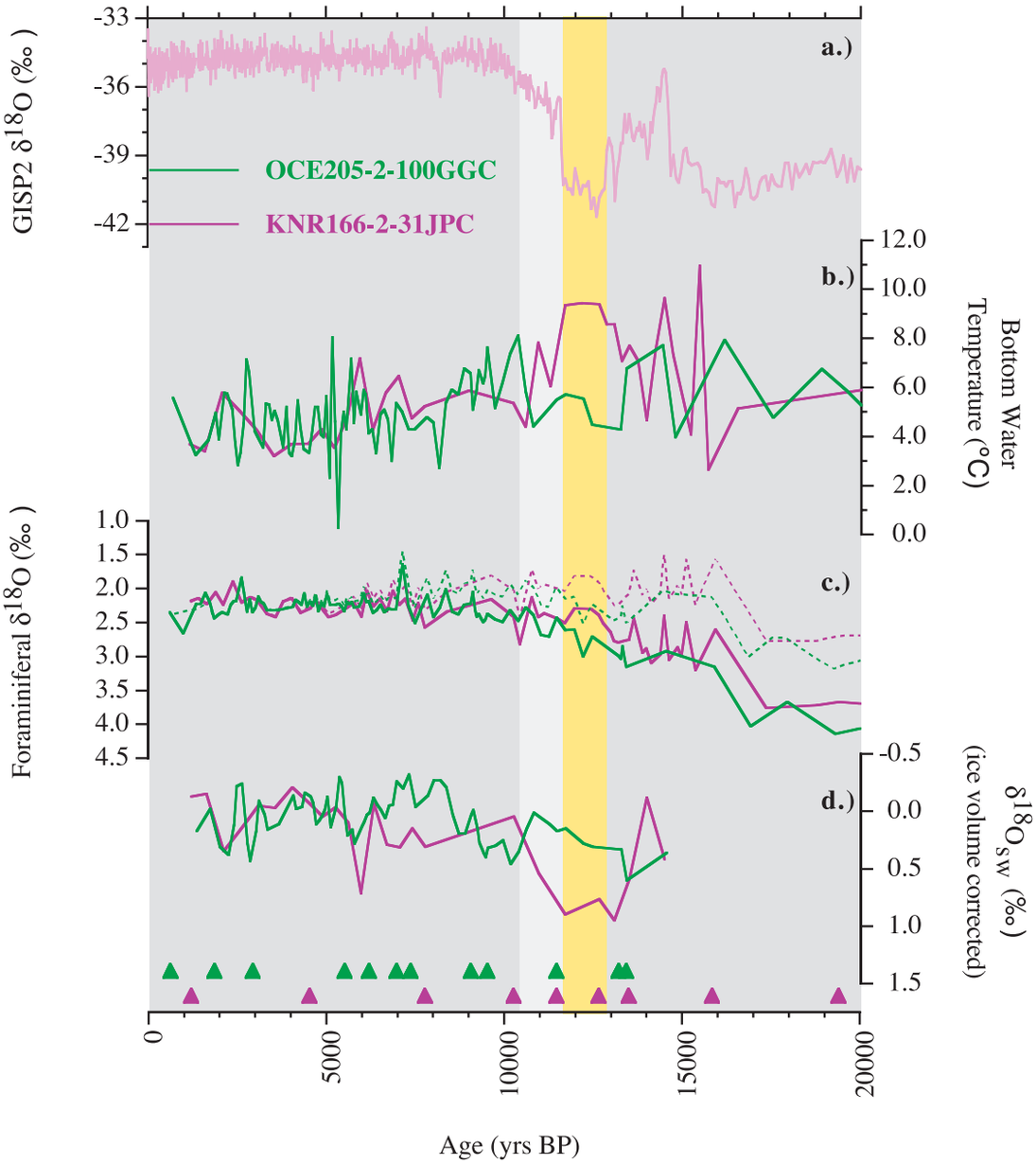

Plate 1. Benthic temperatures and $\delta^{18}O_{sw}$ from OCE205-2-100GGC and KNR166-2-31JPC vs. calendar age. (a) GISP2 $\delta^{18}O$ (pink) [*Grootes et al.*, 1993]; (b) average Mg/Ca-derived temperatures for 100GGC (green) and 31JPC (purple); (c) average benthic foraminiferal $\delta^{18}O$ for 100GGC (green) [*Slowey and Curry*, 1995; this paper] and 31JPC (purple); dashed lines are $\delta^{18}O$ corrected for ice-volume change using *Waelbroeck et al*. [2002]; (d) $\delta^{18}O_{sw}$ calculated using 3-point smoothed Mg/Ca-derived temperatures, 3-point smoothed ice-volume corrected foraminiferal $\delta^{18}O$, and the $\delta^{18}O$-temperature equation for *Cibicidoides* spp.: $\delta^{18}O_{Cib} = [\delta^{18}O_{sw} - 0.27] - 0.21BWT + 3.38$ [*Lynch-Stieglitz et al.*, 1999]. Triangles (green and purple, respectively, as above) are AMS dates converted to calendar age. Yellow shading marks the Younger Dryas interval.

Comparison of the two intermediate depth records reveals similar temperatures at LBB and FC throughout much of the last 20,000 years. In particular, BWTs were comparable before the Younger Dryas and after 10.5 ka. However, at ~14 ka (prior to the Younger Dryas cooling over Greenland), temperatures at the two sites began to diverge, perhaps in response to an increase in meltwater during the interval 15.6-14.3 ka [*Licciardi et al*., 1999]. Our data suggest an increased temperature gradient between the two sites, with BWTs 4°C warmer at FC than at LBB. After the end of the Younger Dryas event, the temperature difference between the two sites remained Younger Dryas–like for ~1 kyr. By ~10.5 ka, temperatures at the two sites converged, and a horizontal temperature gradient similar to the modern was established.

BENTHIC FORAMINIFERAL $\delta^{18}O$ AND $\delta^{18}O_{sw}$ RESULTS

Previously acquired [*Slowey and Curry*, 1995] and newly acquired [this paper] benthic $\delta^{18}O$ results from LBB, and newly acquired benthic $\delta^{18}O$ results from FC are presented in Figures 2c and 3c and Plate 1c. Glacial-interglacial trends are present in the $\delta^{18}O$ records from both cores. At LBB, $\delta^{18}O$ shifts from 4.1‰ during the last glacial to 2.4‰ during the Holocene. At FC, $\delta^{18}O$ shifts from 3.7‰ to 2.2‰. Values at the two sites are offset from each other by about 0.5‰ during the glacial, but converge at ~11.5 ka, and remain very similar for the remainder of the record. Variability during the Younger Dryas is not prominent in either $\delta^{18}O$ record, but three light $\delta^{18}O$ excursions of >0.5‰ are present in the portion of the FC record prior to 13 ka.

Seawater $\delta^{18}O$ was calculated using Eqn 4 and is presented in Plate 1d. Seawater $\delta^{18}O$ was not calculated for samples older than 15,000 years because Mg/Ca analyses and $\delta^{18}O$ analyses were not performed on samples from the same depth intervals. Holocene $\delta^{18}O_{sw}$ values at both LBB and FC are consistent with modern values. At both locations, salinity variability occurred during the Younger Dryas. At LBB, $\delta^{18}O_{sw}$ decreased by ~0.4‰ (a salinity decrease of 0.8 using the modern $\delta^{18}O_{sw}$–salinity relationship). At FC, $\delta^{18}O_{sw}$ increased by ~0.8‰ (a salinity increase of 1.6). Overall, the $\delta^{18}O_{sw}$ data for the two locations suggest similar salinities during most of the record, but an increased salinity gradient during the Younger Dryas, when salinities at FC were significantly higher than at LBB. A similar salinity gradient was also present from ~8.6 to 6.5 ka.

MODEL RESPONSE

In response to a surface freshwater forcing of 0.1 Sv for a period of 100 years, meridional overturning in the GFDL R30 model is greatly reduced from 25 Sv during the control run to about 13 Sv during the experiment (Figure 5). The addition of freshwater into the North Atlantic causes a large decrease in high latitude surface salinities and surface temperatures (Plate 2). As with previous freshwater forcing experiments [*Manabe and Stouffer*, 1997; *Marchal et al.*, 1999; *Rahmstorf*, 1994], surface temperatures in the lower latitudes increase as a result of the reduction in the northward transport of heat via the upper limb of the Atlantic overturning cell.

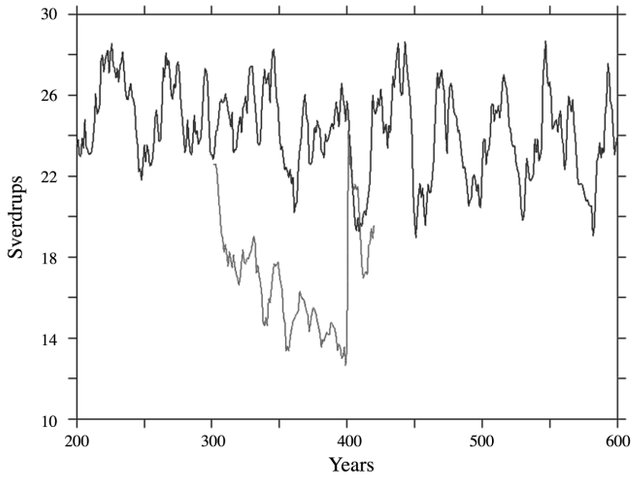

Figure 5. Time-series of the meridional overturning. Black line represents the control integration; gray line represents the 100-year freshwater forcing experiment, which started at year 300 of the control.

The surface stability caused by the freshwater input reduces the strength of deep water formation, but does not cause a cessation of overturning (Plate 3). Instead, convection continues to shallower depths, incorporating the cold, fresh surface waters into the intermediate depth North Atlantic (Plate 4). These cold, fresh waters deflect southwestward due to Coriolis forces, propagating the cooling and freshening anomalies toward the southwestern side of the North Atlantic basin. The resulting decreases in intermediate depth temperatures and salinities are significantly greater in the open ocean North Atlantic than in the eastern Atlantic (Plate 4).

The influence of Mediterranean Outflow Water (MOW) enhances the differences between the intermediate depth anomalies in the open ocean North Atlantic and the eastern Atlantic. MOW is warmer, saltier and denser than other Atlantic waters. When it enters the Atlantic Ocean, it sinks until it reaches the isopycnal surface with the same density (to depths of ~1,000 m in the control run). It then spreads southwestward across the Atlantic along isopycnal surfaces. In the GFDL R30 model, the amount of outflow water entering the Atlantic from the Mediterranean Sea is fixed, but the properties of MOW (such as temperature and salinity) are

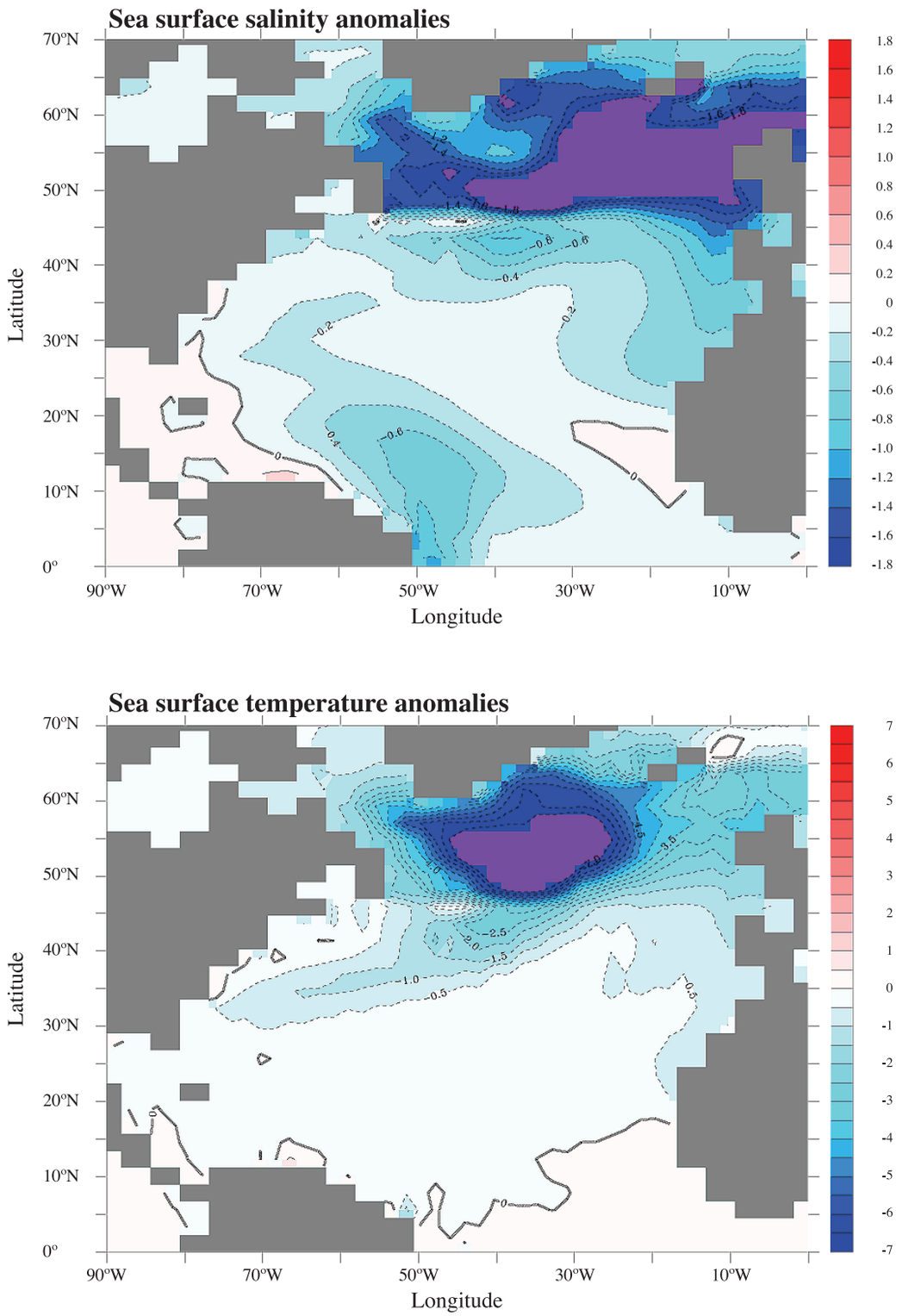

Plate 2. Sea surface anomalies in salinity (upper panel) and temperature (lower panel). Average of years 380-400 of the experiment minus years 300-400 of the control. Purple coloring denotes anomalies that are off the scale.

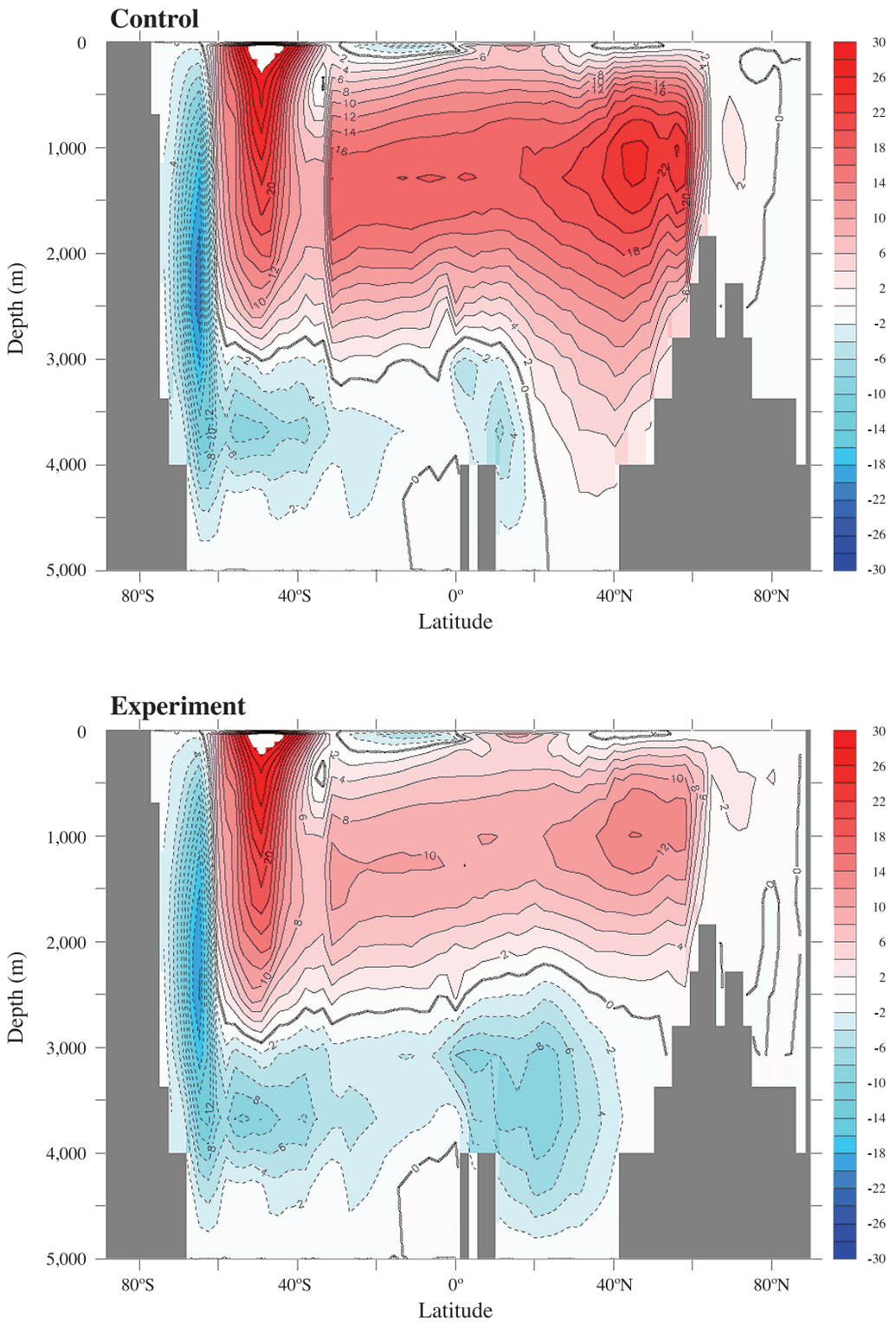

Plate 3. The meridional overturning of the Atlantic Ocean: (upper panel) years 300-400 of the control; (lower panel) years 380-400 of the experiment.

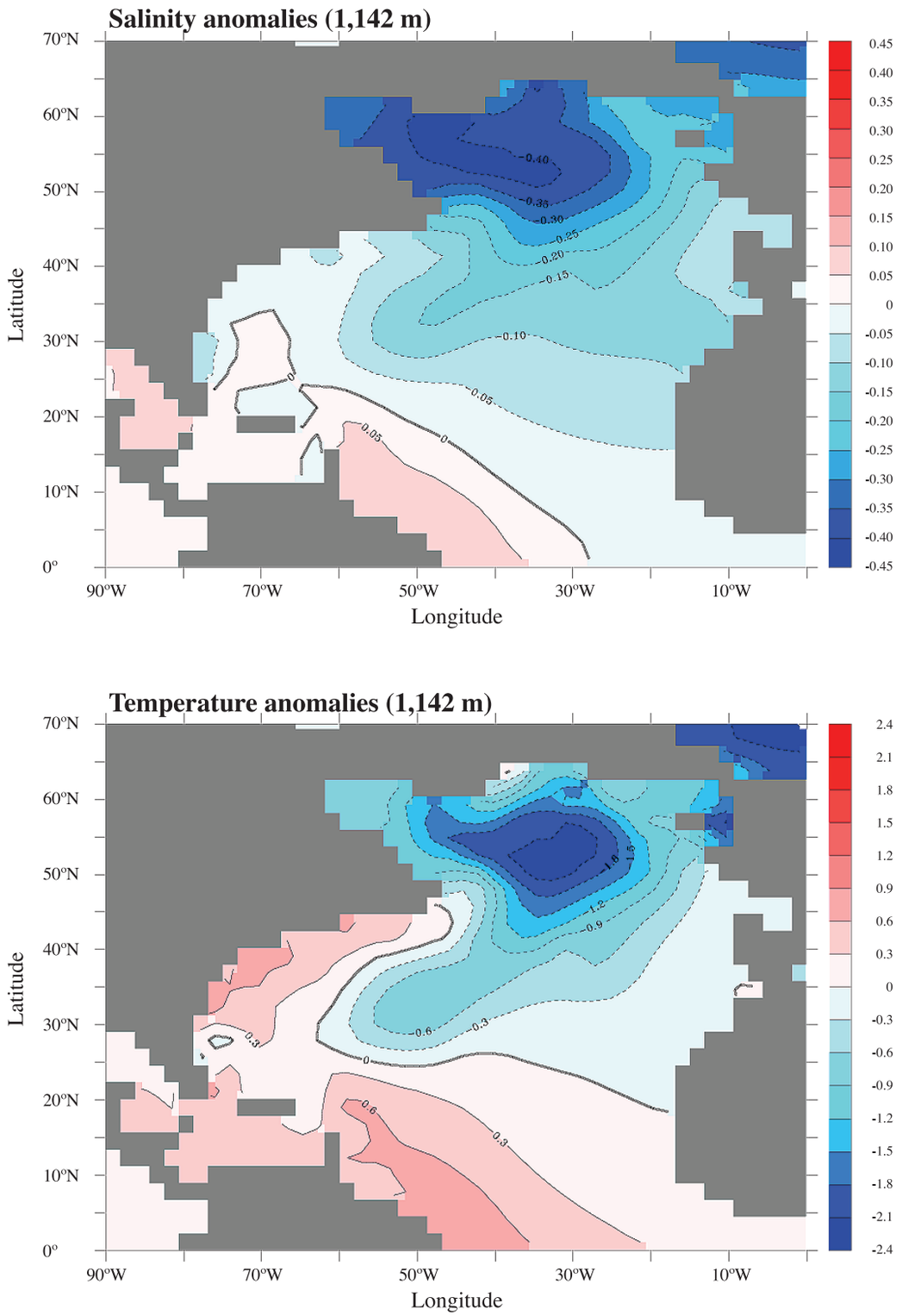

Plate 4. Anomalies at 1,142 m depth in salinity (upper panel) and temperature (lower panel). Average of years 380-400 of the experiment minus years 300-400 of the control.

determined by the gradient between the two water bodies. Therefore, the fresher, colder water in the intermediate depth Atlantic creates stronger gradients between the Atlantic and the Mediterranean, causing increases in the fluxes of salt and heat from the Mediterranean. The result of these increased fluxes is a dampening of the North Atlantic intermediate depth cooling and freshening anomalies in regions affected by MOW.

Plate 4 also reveals a striking contrast between the anomalies in the open ocean Atlantic and those at the western boundary. Waters at the western boundary are significantly warmer and saltier due to the reduced northward transport of heat via the North Atlantic Current, and also due to a southward shift in the location of the Intertropical Convergence Zone [as discussed in detail by *Dahl et al.*, 2005], which causes increased continental runoff from the Amazon River (Plate 2), increased surface stabilities, and decreased upwelling of colder, deeper water.

The model results also show that an overall shoaling of the North Atlantic overturning cell results in increased ventilation in certain parts of the intermediate depth North Atlantic. The negative age anomaly at 1,142 m water depth shows this increased ventilation (Plate 5). The "age" of a parcel of water is set at zero when that parcel has contact with the surface, and the age increases after that parcel leaves the surface. During the last 20 years of the 100-year experiment, the negative age anomaly in the intermediate depth open-ocean North Atlantic is greater than 40 years, signifying younger waters at that depth and a significant increase in ventilation. In eastern parts of the North Atlantic basin, there are regions with little change in the age of the water, and other regions with significant increases in the age of the water, signifying no ventilation change in some eastern regions, and reduced ventilation in others. Superimposed on the age anomaly in Plate 5 are the velocity anomalies for this depth, which emphasize the propagation of temperature, salinity and age anomalies toward the western side of the intermediate depth North Atlantic.

MODEL–DATA COMPARISON

While different in magnitude, the signs of the Younger Dryas temperature variations at the LBB and FC sites are consistent with the results of the freshwater forcing experiment. The model predicts intermediate depth cooling in the open ocean as a result of the incorporation of cool, high latitude surface waters into the subsurface, and LBB, which records intermediate depth variability in the Sargasso Sea, experienced a cooling during the Younger Dryas. The model also predicts warming in the Caribbean at intermediate depths as a result of reduced upwelling and a reduction in the northward transport of heat, and FC, which lies within the northward moving surface return flow of the MOC, experienced a warming during the Younger Dryas. However, the magnitudes of the paleotemperature changes differ significantly from the magnitudes of the model anomalies: model temperature anomalies are on the order of a degree, whereas the data suggest variations on the order of several degrees.

Several factors may contribute to this difference in magnitude. First, the duration of the freshwater forcing experiment was 100 years, versus the ~1,500 year duration of the Younger Dryas. An experiment of longer duration might allow additional cold, fresh surface water to propagate into the subsurface. Second, a freshwater perturbation of the entire North Atlantic region from 50°N to 70°N may not be an appropriate representation of actual forcing, which may have had a point source from the Arctic [*Peltier et al.*, 2006; *Tarasov and Peltier*, 2005], from the Greenland ice sheet [*Jennings et al.*, 2006], or from glacial Lake Agassiz [*Teller et al.*, 2002]. Third, the modern boundary conditions used in this model simulation may not be an adequate representation of the Bølling-Allerød, which was significantly more glaciated than today. And fourth, the coarse resolution of the coupled model may dampen model anomalies.

Alternatively, the slope of the Mg/Ca-temperature calibration may be inadequately defined—an increase in the slope of the calibration line would decrease the variability in the Mg/Ca-derived temperature estimates, thereby increasing agreement between model output and data. Also, the inherent limitations of foraminiferal data quality contribute to the model/data discrepancy.

The signs of the Younger Dryas salinity variations for LBB and FC are also consistent with the model anomalies, but again they are different in magnitude. The model predicts intermediate depth freshening in the open ocean as a result of the incorporation of fresh, high latitude surface waters into the subsurface, and LBB experienced decreased salinities during the Younger Dryas. The model also predicts increased salinities in the Caribbean as a result of reduced transport of high salinity waters from the low latitudes to the high latitudes, and FC, which lies within the northward moving limb of the MOC return flow, experienced increased salinities during the Younger Dryas. However, as with the temperature variations, the magnitudes of the salinity changes in the paleoceanographic data are significantly greater than the magnitudes of the model anomalies: salinity anomalies in the model are on the order of 0.05 to 0.10, whereas the paleoceanographic data from LBB and FC suggest Younger Dryas salinity changes of 0.8 and 1.6, respectively.

COMPARISON WITH OTHER PALEOCEANOGRAPHIC EVIDENCE

The model results predict different intermediate depth ventilation responses in different regions of the North Atlantic: in

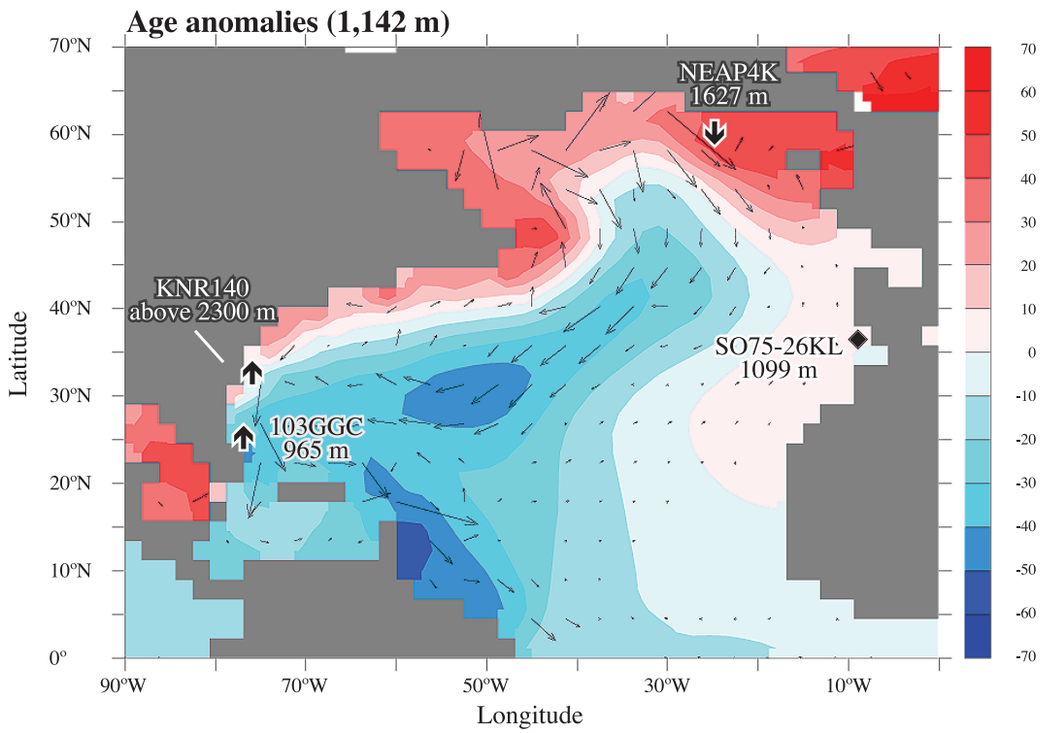

Plate 5. Age tracer anomalies and velocity anomalies at 1,142 m depth. Average of years 380-400 of the experiment minus years 300-400 of the control. Large arrows indicate either increased or decreased Younger Dryas ventilation at the following intermediate depth sites: NEAP4K (61°29'N, 24°10'W, 1,627 m) [*Rickaby and Elderfield*, 2005]; SO75-26KL (37°49'N, 09°30'W, 1,099 m) [*Zahn et al.*, 1997]; KNR140 (various cores above 2,300 m water depth) [*Keigwin*, 2004]; OCE205-2-103GGC (965 m) [*Marchitto et al.*, 1998].

the western subtropics the model results exhibit increased ventilation, but in much of the eastern high latitudes the model results exhibit decreased ventilation (Plate 5). Nutrient evidence from LBB [*Marchitto et al.*, 1998] and benthic-planktic radiocarbon pairs from the Blake Plateau [*Keigwin*, 2004] both suggest increased intermediate depth ventilation during the Younger Dryas, consistent with the model results for the western subtropical Atlantic. On the eastern side of the Atlantic, nutrient evidence from the Portuguese margin [*Zahn et al.*, 1997] suggests no significant change in intermediate depth ventilation during the Younger Dryas, consistent with the model results for this region of the eastern Atlantic. However, for Heinrich events, nutrient evidence from the same Portuguese margin core suggests significantly reduced ventilation [*Zahn et al.*, 1997], underscoring the complexity of the intermediate depth response in the eastern North Atlantic. In the high latitude North Atlantic (Björn Drift), nutrient evidence suggests strongly reduced ventilation during the Younger Dryas [*Rickaby and Elderfield*, 2005], also consistent with the increased ages predicted by the model for the high latitudes. Thus, the model results provide one possible explanation for the apparent differences among records of the Younger Dryas from various intermediate depth regions of the North Atlantic.

The model results are also consistent with paleoceanographic evidence from the deep North Atlantic. Foraminiferal Cd/Ca evidence from the Bermuda Rise [*Boyle and Keigwin*, 1987] indicates a decrease in the influence of northern source waters in the deep North Atlantic during the Younger Dryas, while evidence from the Florida Strait [*Came et al.*, 2007] indicates a concomitant decrease in the influence of southern source waters within the northward return flow of the MOC. These paleoceanographic changes in water mass distribution are consistent with the hypothesis of a reduced MOC during the Younger Dryas, and they are consistent with the model response to freshwater forcing. Foraminiferal $\delta^{13}C$ also suggest a decrease in the influence of northern source waters in the deep North Atlantic during the Younger Dryas [*Austin and Kroon*, 2001; *Keigwin and Lehman*, 1994], although a core from the Feni Drift [*Jansen and Veum*, 1990] does not experience a significant reduction in the influence of northern source waters. However, the Feni Drift core is located at 2,300 m water depth, and it may record variability in an upper component of North Atlantic source waters, which may have become more ventilated during the Younger Dryas [*Marchitto et al.*, 1998; *Zahn and Stüber*, 2002; this paper]. In addition, evidence from benthic planktic radiocarbon pairs [*Keigwin*, 2004; *Robinson et al.*, 2005], and the dynamic tracer Pa/Th [*McManus et al.*, 2004], which records changes in overturning rather than changes in water mass origin, confirm the results obtained using passive nutrient tracers.

CONCLUSION: AN EMERGING PICTURE FOR THE YOUNGER DRYAS

Several zonally averaged models predict intermediate depth warming in response to North Atlantic freshwater forcing; however, this is the first study to compare the spatial distribution of simulated temperature and salinity anomalies at intermediate depth to paleoceanographic data. The model results reveal a more complex pattern of intermediate depth variability than can be predicted with a zonally averaged representation. The results indicate cooling and freshening of the open-ocean North Atlantic, and warming and increased salinities at the western boundary, consistent with our two new Younger Dryas temperature and salinity records, and consistent with a previous intermediate depth temperature record from the tropics [*Rühlemann et al.*, 2004]. In addition, the model results are consistent with other paleoceanographic data suggesting increased intermediate depth ventilation during the Younger Dryas [*Keigwin*, 2004; *Marchitto et al.*, 1998; *Zahn and Stüber*, 2002] and provide a possible explanation for the apparent discrepancies between data from various regions of the North Atlantic, such as strongly reduced ventilation in the very high latitudes and in the eastern Atlantic during the Younger Dryas and during Heinrich events [*Rickaby and Elderfield*, 2005; *Zahn et al.*, 1997].

The results, taken together with the results from previous paleoceanographic studies, reveal an emerging picture of Younger Dryas subsurface geometry, in which well-ventilated, North Atlantic intermediate waters flow southward over poorly ventilated northward-flowing deep waters, similar to the subsurface geometry during the last glacial. The agreement between the growing body of paleoceanographic evidence and the response of the GFDL R30 coupled ocean-atmosphere general circulation model to a North Atlantic freshwater forcing suggests that freshwater is a possible driver or amplifier of Bølling-Allerød to Younger Dryas climate variability. However, the model–data agreement does not rule out the possibility of an alternative forcing mechanism that could create the same spatial and temporal distribution of temperature, salinity, radiocarbon, Pa/Th, Cd_W, and $\delta^{13}C$ variability. An examination of all the paleoceanographic evidence in the context of a southern hemisphere freshwater forcing experiment would help to clarify our understanding of the types of forcing mechanisms that could be consistent with the paleoceanographic evidence.

Acknowledgments. We thank Yair Rosenthal and Simon Thorrold for helpful discussions; Rong Zhang and an anonymous reviewer for comments; and D. Ostermann, S. Birdwhistell, L. Baker and H. Griffiths for laboratory assistance. Funding was provided by the WHOI Ocean and Climate Change Institute, Agricultural Experiment Station Project NJ07167, and NSF grants OCE0096495,

ATM0502428, OCE0096472, OCE0220776, and ATM0501351. The cores used in this study are archived at the WHOI core repository, which is supported by the NSF.

REFERENCES

Andrews, J.T., A.E. Jennings, M. Kerwin, M. Kirby, W. Manley, and G.H. Miller, A Heinrich-like event, H-0 (DC-0): Source(s) for detrital carbonate in the North Atlantic during the Younger Dryas chronozone, *Paleoceanography*, 10, 943-952, 1995.

Austin, W.E.N., and D. Kroon, Deep sea ventilation of the northeastern Atlantic during the last 15,000 years, *Global Planet. Change*, 30, 13-31, 2001.

Bond, G., W.S. Broecker, S. Johnsen, J.F. McManus, L.D. Labeyrie, J. Jouzel, and G. Bonani, Correlations between climate records from North Atlantic sediments and Greenland ice, *Nature*, 365, 143-147, 1993.

Bond, G.C., and R. Lotti, Iceberg discharges into the North Atlantic on millennial time scales during the last deglaciation, *Science*, 267, 1005-1010, 1995.

Boyle, E.A., Manganese carbonate overgrowths on foraminifera tests, *Geochim. Cosmochim. Acta*, 47, 1815-1819, 1983.

Boyle, E.A., and L.D. Keigwin, Comparison of Atlantic and Pacific paleochemical records for the last 215,000 years: changes in deep ocean circulation and chemical inventories, *Earth Planet. Sci. Lett.*, 76, 135-150, 1985/6.

Boyle, E.A., and L.D. Keigwin, North Atlantic thermohaline circulation during the past 20,000 years linked to high-latitude surface temperature, *Nature*, 330, 35-40, 1987.

Boyle, E.A., L.D. Labeyrie, and J.-C. Duplessy, Calcitic foraminiferal data confirmed by cadmium in aragonitic Hoeglundina: Application to the Last Glacial Maximum in the northern Indian Ocean, *Paleoceanography*, 10, 881-900, 1995.

Boyle, E.A., and Y. Rosenthal, Chemical hydrography of the South Atlantic during the Last Glacial Maximum: Cd and $\delta^{13}C$, in *The South Atlantic: Present and Past Circulation*, edited by G. Wefer, pp. 423-443, Springer-Verlag, Berlin, 1996.

Broecker, W.S., J.P. Kennett, B.P. Flower, J.T. Teller, S. Trumbore, G. Bonani, and W. Wolfli, Routing of meltwater from the Laurentide ice-sheet during the Younger Dryas cold episode, *Nature*, 341, 318-321, 1989.

Broecker, W.S., and T.-H. Peng, *Tracers in the Sea*, 690 pp., Lamont-Doherty Earth Obs., Palisades, NY, 1982.

Bryan, K., and L.J. Lewis, water mass model of the World Ocean, *J. Geophys. Res.*, 84, 2503–2517, 1979.

Came, R.E., D.W. Oppo, and W.B. Curry, Atlantic Ocean circulation during the Younger Dryas: Insights from a new Cd/Ca record from the western subtropical South Atlantic, *Paleoceanography*, 18, 1086, doi:1010.1029/2003PA000888, 2003.

Came, R.E., D.W. Oppo, W.B. Curry, and J. Lynch-Stieglitz, Variability in the influence of southern source water in the Florida Current since the last glacial, *Paleoceanography* 2007.

Dahl, K.A., A.J. Broccoli, and R.J. Stouffer, Assessing the role of North Atlantic freshwater forcing in millennial scale climate variability: a tropical Atlantic perspective, *Clim. Dyn.*, 24, 325-346, 2005.

Dansgaard, W., North Atlantic climate oscillations revealed by deep Greenland ice cores, in *Climate Processes and Climate Sensitivity, Geophysical Monograph Series,* 29, edited by J.E. Hanson and T. Takahashi, p. 288–298, American Geophysical Union, Washington, D.C, 1984.

Dansgaard, W., et al., Evidence for general instability of past climate from a 250-Kyr ice-core record, *Nature*, 364, 218-220, 1993.

Delworth, T.L., R.J. Stouffer, K.W. Dixon, M.J. Spelman, T.R. Knutson, A.J. Broccoli, P.J. Kushner, and R.T. Wetherald, Review of simulations of climate variability and change with the GFDL R30 coupled climate model, *Clim. Dyn.*, 19, 555-574, 2002.

Duplessy, J.-C., N.J. Shackleton, R.G. Fairbanks, L.D. Labeyrie, D.W. Oppo, and N. Kallel, Deep water source variations during the last climatic cycle and their impact on the global deep water circulation, *Paleoceanography*, 3, 343-360, 1988.

Gordon, A.L., Interocean exchange of thermocline water, *J. Geophys. Res.*, 91, 5037-5046, 1986.

Grootes, P.M., M. Stuiver, J.W.C. White, S.J. Johnsen, and J. Jouzel, Comparison of oxygen-isotope records from the GISP2 and GRIP Greenland ice cores, *Nature*, 366, 552-554, 1993.

Hughen, K.A., et al., Marine04 marine radiocarbon age calibration, 0–26 cal kyr BP, *Radiocarbon*, 46, 1059-1086, 2004.

Jansen, E., and T. Veum, Evidence for two-step deglaciation and its impact on North Atlantic deep-water circulation, *Nature*, 343, 612-616, 1990.

Jenkins, W.J., Tritium and He-3 in the Sargasso Sea, *J. Mar. Res.*, 38, 533-569, 1980.

Jennings, A.E., M. Hald, M. Smith, and J.T. Andrews, Freshwater forcing from the Greenland Ice Sheet during the Younger Dryas: evidence from southeastern Greenland shelf cores, *Quat. Sci. Rev.*, 25, 282-298, 2006.

Keeling, R.F., and B.B. Stephens, Antarctic sea ice and the control of Pleistocene climate instability, *Paleoceanography*, 16, 112-131, 2001.

Keigwin, L.D., Radiocarbon and stable isotope constraints on Last Glacial Maximum and Younger Dryas ventilation in the western North Atlantic, *Paleoceanography*, 19, PA4012, doi:4010.1029/2004PA001029, 2004.

Keigwin, L.D., G.A. Jones, S.J. Lehman, and E.A. Boyle, Deglacial meltwater discharge, North-Atlantic deep circulation, and abrupt climate change, *J. Geophys. Res.*, 96, 16811-16826, 1991.

Keigwin, L.D., and S.J. Lehman, Deep circulation change linked to Heinrich Event-1 and Younger Dryas in a middepth North-Atlantic core, *Paleoceanography*, 9, 185-194, 1994.

Lea, D.W., D.K. Pak, L.C. Peterson, and K.A. Hughen, Synchroneity of tropical and high-latitude Atlantic temperatures over the last glacial termination, *Science*, 301, 1361-1364, 2003.

Lehman, S.J., and L.D. Keigwin, Sudden changes in North-Atlantic circulation during the last deglaciation, *Nature*, 356, 757-762, 1992.

Levitus, S., and T. Boyer, *World Ocean Atlas 1994 Volume 4: Temperature. NOAA Atlas NESDIS 4*, U.S. Department of Commerce, Washington, D.C, 1994.

Licciardi, J.M., J.T. Teller, and P.U. Clark, Freshwater routing by the Laurentide ice sheet during the last deglaciation, in *Mechanisms of Global Climate Change at Millennial Time Scales, Geophysical Monograph Series,* 112, edited by P.U. Clark, et al., pp. 177-201, American Geophysical Union, Washington, D.C, 1999.

Luyten, J.R., J. Pedlosky, and H. Stommel, The ventilated thermocline, *J. Phys. Oceanogr.*, 13, 192-309, 1983.

Lynch-Stieglitz, J., W.B. Curry, and N.C. Slowey, A geostrophic transport estimate for the Florida Current from the oxygen isotope composition of benthic foraminifera, *Paleoceanography*, 14, 360-373, 1999.

Manabe, S., and R.J. Stouffer, Coupled ocean-atmosphere model response to freshwater input: Comparison to Younger Dryas event, *Paleoceanography*, 12, 321-336, 1997.

Marchal, O., T.F. Stocker, and F. Joos, Physical and biogeochemical responses to freshwater induced thermohaline variability in a zonally averaged ocean model, in *Mechanisms of Global Climate Change at Millennial Time Scales, Geophysical Monograph Series,* 112, edited by P.U. Clark, et al., pp. 263-284, American Geophysical Union, Washington, D.C, 1999.

Marchitto, T.M., W.B. Curry, and D.W. Oppo, Millennial-scale changes in North Atlantic circulation since the last glaciation, *Nature*, 393, 557-561, 1998.

McCartney, M.S., The subtropical recirculation of mode waters, *J. Mar. Res.*, 40, *suppl.*, 427-464, 1982.

McManus, J.F., R. Francois, J.M. Gherardi, L.D. Keigwin, and S. Brown-Leger, Collapse and rapid resumption of Atlantic meridional circulation linked to deglacial climate changes, *Nature*, 428, 834-837, 2004.

Oppo, D.W., and S.J. Lehman, Mid-Depth circulation of the subpolar North Atlantic during the Last Glacial Maximum, *Science*, 1148-1152, 1993.

Peltier, W.R., G. Vettoretti, and M. Stastna, Atlantic meridional overturning and climate response to Arctic Ocean freshening, *Geophys. Res. Lett.*, 33, L06713, doi:06710.01029/02005GL025251, 2006.

Rahmstorf, S., Rapid climate transitions in a coupled ocean-atmosphere model, *Nature*, 372, 82-85, 1994.

Redi, M.H., Oceanic isopycnal mixing by coordinate rotation, *J. Phys. Oceanogr.*, 12, 1154–1158, 1982.

Rickaby, R.E.M., and H. Elderfield, Evidence from the high-latitude North Atlantic for variations in Antarctic Intermediate water flow during the last

deglaciation, *Geochem. Geophys. Geosys.*, 6, Q05001, doi:05010.01029/02004GC000858, 2005.

Robinson, L.F., J.F. Adkins, L.D. Keigwin, J. Southon, D.P. Fernandez, S.-L. Wang, and D.S. Scheirer, Radiocarbon variability in the western North Atlantic during the last deglaciation, *Science*, 310, 1469-1473, 2005.

Rosenthal, Y., *Late quaternary paleochemistry of the Southern Ocean: Evidence from cadmium variablity in sediments and foraminifera*, 186 pp., Massachusetts Institute of Technology and Woods Hole Oceanographic Institution, PhD Thesis, Woods Hole, MA.

Rosenthal, Y., M.P. Field, and R.M. Sherrell, Precise determination of element/calcium ratios in calcareous samples using sector field inductively coupled plasma mass spectrometry, *Anal. Chem.*, 71, 3248-3253, 1999.

Rosenthal, Y., P. Lam, E.A. Boyle, and J. Thomson, Authigenic cadmium enrichments in suboxic sediments: Precipitation and postdepositional mobility, *Earth Planet. Sci. Lett.*, 132, 99-111, 1995.

Rosenthal, Y., C.H. Lear, D.W. Oppo, and B. Linsley, Temperature and carbonate ion effects on Mg/Ca and Sr/Ca ratios in benthic foraminifera: Aragonitic species *Hoeglundina elegans*, *Paleoceanography*, 21, PA1007, doi:1010.1029/2005PA001158, 2006.

Ruddiman, W.F., and A. McIntyre, The North Atlantic Ocean during the last deglaciation, *Palaeogeogr. Paleoclimatol. Paleoecol.*, 35, 145-214, 1981.

Rühlemann, C., S. Mulitza, G. Lohmann, A. Paul, M. Prange, and G. Wefer, Intermediate depth warming in the tropical Atlantic related to weakened thermohaline circulation: Combining paleoclimate data and modeling results for the last deglaciation, *Paleoceanography*, 19, PA1025, doi:1010.1029/2003PA000948, 2004.

Rühlemann, C., S. Mulitza, P.J. Muller, G. Wefer, and R. Zahn, Warming of the tropical Atlantic Ocean and slowdown of thermohaline circulation during the last deglaciation, *Nature*, 402, 511-514, 1999.

Saenko, O.A., A.J. Weaver, and J.M. Gregory, On the link between the two modes of the ocean thermohaline circulation and the formation of global-scale water masses, *J. Clim.*, 16, 2797-2801, 2003a.

Saenko, O.A., A.J. Weaver, and A. Schmittner, Atlantic deep circulation controlled by freshening in the Southern Ocean, *Geophys. Res. Lett.*, 30, 1754, doi:1710.1029/2003GL017681, 2003b.

Sarmiento, J.L., C.G. Rooth, and W. Roether, The North Atlantic tritium distribution in 1972, *J. Geophys. Res.*, 87, 8047-8056, 1982.

Sarnthein, M., et al., Fundamental modes and abrupt changes in North Atlantic circulation and climate over the last 60 kyr—Concepts, reconstruction and numerical modeling, in *The Northern North Atlantic: A Changing Environment*, edited by P. Schafer, et al., pp. 365-410, Springer-Verlag, New York, 2001.

Schmitz, W.J., J.R. Luyten, and R.W. Schmitt, On the Florida Current T/S envelope, *Bull. Mar. Sci.*, 53, 1048-1065, 1993.

Schmitz, W.J., and P.L. Richardson, On the sources of the Florida Current, *Deep-Sea Res.*, 38, S379-S409, 1991.

Slowey, N.C., and W.B. Curry, Glacial-interglacial differences in circulation and carbon cycling within the upper western North-Atlantic, *Paleoceanography*, 10, 715-732, 1995.

Stouffer, R.J., et al., Investigating the causes of the response of the thermohaline circulation to past and future climate changes, *J. Clim.*, 19, 1365-1387, 2006.

Stuiver, M., and P.J. Reimer, Extended ^{14}C database and revised CALIB radiocarbon calibration program, *Radiocarbon*, 35, 215-230, 1993.

Tarasov, L., and W.R. Peltier, Arctic freshwater forcing of the Younger Dryas cold reversal, *Nature*, 435, 662-665, 2005.

Teller, J.T., D.W. Leverington, and J.D. Mann, Freshwater outbursts to the oceans from glacial Lake Agassiz and their role in climate change during the last deglaciation, *Quat. Sci. Rev.*, 21, 879-887, 2002.

Thompson, L.G., et al., A 25,000-year tropical climate history from Bolivian ice cores, *Science*, 282, 1858-1864, 1998.

Waelbroeck, C., L. Labeyrie, E. Michel, J.-C. Duplessy, J.F. McManus, K. Lambeckd, E. Balbona, and M. Labracherie, Sea-level and deep water temperature changes derived from benthic foraminifera isotopic records, *Quat. Sci. Rev.*, 21, 295-305, 2002.

Weldeab, S., R.R. Schneider, and M. Kölling, Deglacial sea surface temperature and salinity increase in the western tropical Atlantic in synchrony with high latitude climate instabilities, *Earth Planet. Sci. Lett.*, 241, 699-706, 2006.

Wang, Y.J., H. Cheng, R.L. Edwards, Z.S. An, J.Y. Wu, C.C. Shen, and J.A. Dorale, A high-resolution absolute-dated Late Pleistocene monsoon record from Hulu Cave, China, *Science*, 294, 2345-2348, 2001.

Weaver, A.J., O.A. Saenko, P.U. Clark, and J. Mitrovica, Meltwater pulse 1A from Antarctica as a trigger of the Bølling-Allerød warm interval, *Science*, 299, 1709-1713, 2003.

Zahn, R., J. Schonfeld, H.R. Kudrass, M.H. Park, H. Erlenkeuser, and P.M. Grootes, Thermohaline instability in the North Atlantic during meltwater events: Stable isotope and ice-rafted detritus records from core SO75-26KL, Portuguese margin, *Paleoceanography*, 12, 696-710, 1997.

Zahn, R., and A. Stüber, Suborbital intermediate water variability inferred from paired benthic foraminiferal Cd/Ca and $\delta^{13}C$ in the tropical West Atlantic and linking with North Atlantic climates, *Earth Planet. Sci. Lett.*, 200, 191-205, 2002.

Zhang, R., and T.L. Delworth, Simulated Tropical Response to a Substantial Weakening of the Atlantic Thermohaline Circulation, *J. Clim.*, 18, 1853-1860, 2005.

A. J. Broccoli, Department of Environmental Sciences, Rutgers University, New Brunswick, New Jersey, USA.

R. E. Came, Division of Geological and Planetary Sciences, California Institute of Technology, Pasadena, California, USA. (rcame@gps.caltech.edu)

W. B. Curry and D. W. Oppo, Department of Geology and Geophysics, Woods Hole Oceanographic Institution, Woods Hole, Massachusetts, USA.

J. Lynch-Stieglitz, School of Earth and Atmospheric Sciences, Georgia Institute of Technology, Atlanta, Georgia, USA.

R. J. Stouffer, NOAA Geophysical Fluid Dynamics Laboratory, Princeton, New Jersey, USA.